

## UNCERTAINTY IN CMMs

**Rosenda Valdés Arencibia**, [arvaldes@mecanica.ufu.br](mailto:arvaldes@mecanica.ufu.br)

Universidade Federal de Uberlândia. FEMEC. Av. João Naves de Ávila, 2121 – Bloco 1M, Uberlândia - MG, CEP 38400-902

**Denise Pizarro Vieira Sato**, [denise@4all.com.br](mailto:denise@4all.com.br)

Unifei. Av. Humberto de A. C. Branco, 3972 - São Bernardo do Campo - SP- CEP: 09850-901.

**Olívio Novaski**, [novaski@fem.unicamp.br](mailto:novaski@fem.unicamp.br)

DEF/FEM/UNICAMP Caixa Postal 6122 - Campinas (SP). CEP: 13083-860

**Benedito Di Giacomo**, [bgiacomo@sc.usp.br](mailto:bgiacomo@sc.usp.br)

Escola de Engenharia de São Carlos. USP. Av. Trabalhador São-carlense N.400 Bairro Centro. São Carlos. SP. CEP: 13566-590

**Abstract:** *The aim of the present work is to calculate the uncertainty associated with volumetric error components in a Moving Bridge type Coordinate Measuring Machine (CMM). The methodology developed consisted in equationing the components of the volumetric error using homogeneous transformations techniques; application of the law of uncertainty propagation, according to the recommendation of ISO GUM, 1993, in the obtained synthesization equations and measurement of the geometric errors and Abbè offsets by means of the direct calibration method. Instruments such as the laser interferometer and the mechanical square standard were used. After measurement, mathematical models regarding each geometric error and Abbè offset were written and the law of uncertainty propagation was applied, again, for each of the obtained equations for determining the uncertainty. The mathematical models considered all the variables of influence and correction factors. As conclusions it may be stated that at any point in the work volume of the CMM, the components of volumetric error of X, Y and Z axes present uncertainty values close to 2,7, 4,0 and 2,0  $\mu\text{m}$ , respectively.*

**Key words:** *Standard uncertainty; geometric error; Abbé offset.*

### 1. INTRODUCTION

Every result of measurement is only an estimate of true value. This is due to the influence of several factors that interfere in the measurement process, such as variations associated to the measurement instrument, to the operator, to the environment and other conditions. The difference between conventional true value and indicated value in a measurement is denominated measurement errors. In many measurement processes the conventional true value is unknown; therefore, the measurement error is calculated by the difference between the result of measurement and the indicated value through calibration.

According to its behavior, the measurement error can be classified as systematic or random. When none of the causes that provoke the random errors is predominant, one can say that its occurrence and behavior coincide with the normal probability curve or Gaussian distribution curve. Therefore, it can be assumed that the random errors follow the law of normal distribution. However, not all of the sources of errors in a measurement process present normal probability distributions. There are, for example, rectangular, trapezoidal and triangular distributions.

Systematic effects can be corrected without great difficulties; nevertheless, after the correction, a doubt will still remain about how well corrected the value obtained in a measurement is. By adding this doubt to those of systematic and random effects, the conventionally so called measurement uncertainty (ISO GUM, 1993) can be obtained.

The word uncertainty means doubt, and thus the doubt about the validity of the result of a measurement is called measurement uncertainty. The uncertainty of the measurement result reflects the lack of exact knowledge of the measured value. At the present time, it is not enough to express the numerical value of the measured errors, arising thus, the need to indicate quantitatively the quality of the result of a measurement. In other words, adding to the result of the measurement a statement about the reliability associated to it, that is, the measurement uncertainty.

According to the (ISO GUM, 1993), the measurement uncertainty can be defined as being the parameter, associated to the result of a measurement that characterizes the dispersion of the values that could reasonably be attributed to the quantity. Such parameter may be the standard deviation or multiple of it, or the half-width of an interval corresponding to a given level of reliability.

### 2. MEASUREMENT UNCERTAINTY IN CMMs

The evaluation of measuring instruments, such as Coordinate Measuring Machines through measurement uncertainty, is a rather difficult task due to the large number of factors that can contribute to the uncertainty, as well as the machine versatility, which allows measuring several metrological features of a workpiece (Balsamo, 1999).

The Coordinate Measuring Machines are fast, accurate, flexible and reliable quality control means. Nevertheless, the performance of these machines has been limited by several factors, which act together, combining complex ways throughout the working volume of the machine, generating the called volumetric error. The largest contribution to the volumetric error is constituted by geometric errors (Bosch, 1995). These errors have their origin in the geometric deviations of the different components of the Measuring Machine, and they appear during the movement of the coordinate axes, due to the interaction among the components.

In order to study geometric errors, the CMM moving elements are assumed as rigid bodies. The position of a rigid body in space can be defined by six degrees of freedom. Since each degree of freedom can be associated to an error, six geometric errors are associated to each preferential axis of the CMM, specifically, one position error, two straightness errors and three rotation errors (pitch, yaw and roll), summing up a total number of 18 geometric errors. Three more errors must be added due to the impossibility of arranging three perfectly orthogonal axes, namely orthogonal errors, which depend on the relation between components. Therefore, a full amount of 21 errors can be determined from three Cartesian axes CMMs. Complex combinations of geometric errors in the work volume of the CMM generate the components of the volumetric error.

It is known that inspections using CMMs are carried out from coordinate points ( $X_i$ ,  $Y_i$  and  $Z_i$ ) on a given surface. The coordinates of the points, which are measured by means of an optical-electronic system, are used by the CMM software to identify the geometric features of the workpiece. The real coordinates of the points in the CMM work volume can be determined if the measured coordinates and their respective errors are known, Eq. (1).

$$\begin{aligned} X_{Real} &= X_{Machine} - E_x \\ Y_{Real} &= Y_{Machine} - E_y \\ Z_{Real} &= Z_{Machine} - E_z \end{aligned} \quad (1)$$

where:  $X_{Machine}$ ,  $Y_{Machine}$  and  $Z_{Machine}$  are the coordinates of the measured points;  $X_{Real}$ ,  $Y_{Real}$  and  $Z_{Real}$  are the ideal or true coordinates and  $E_x$ ,  $E_y$  and  $E_z$  are the error components associated to each coordinate.

The uncertainty associated to the real coordinates ( $X_{Real}$ ,  $Y_{Real}$  and  $Z_{Real}$ ) can be assumed as being equal to zero and the uncertainty associated to coordinates  $X$ ,  $Y$  and  $Z$  of the measured points can be considered equal to the uncertainty obtained for the components of the volumetric error,  $E_x$ ,  $E_y$  and  $E_z$ , Eq. (2).

$$\begin{aligned} u(X_{Machine}) &= u(E_x) \\ u(Y_{Machine}) &= u(E_y) \\ u(Z_{Machine}) &= u(E_z) \end{aligned} \quad (2)$$

Therefore, the uncertainty of three-dimensional measurement can be determined from the uncertainties associated to the spatial points that define the sought dimensional feature. Such uncertainty is referred to as three-dimensional or volumetric and is related to a region in space whose shape and size are defined by the combination of the various existing uncertainty sources, Fig. 1.

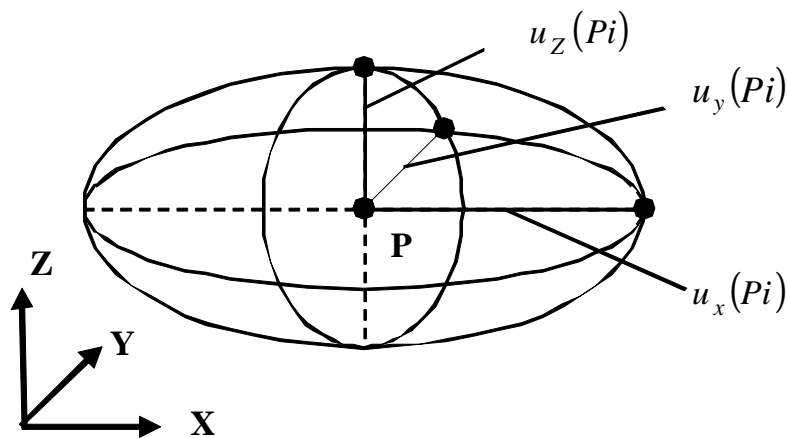


Figure 1. Representation of three-dimensional uncertainty.

This work presents a methodology to estimate the measurement uncertainty associated to the components of the volumetric error of a moving bridge CMM, aiming, in the future, at the determination of the measurement uncertainty associated to the measurements performed with these machines. All experimental runs for the acquisition of error data were conducted on a Moving Bridge CMM at the Metrology Laboratory, University of São Paulo, Brazil (Fig. 2).

The machine consists of a cast aluminium structure with the shape of a bridge that moves with relation to a granite flat surface. The workpieces are attached to the flat surface by means of screws, clamps and fixtures. The flat surface is mounted on balls over vee-blocks on the steady structure of the machine. Three sets of aerostatic bearings provide the movement of axes X, Y and Z over the slideways. The bearings require dry and clean compressed air to produce the layer that sustains the moving parts of the structure.



Figure 2. Moving Bridge type CMM.

## 2.1. Geometric model

The error synthesization model used to estimate uncertainty measurement associated volumetric components errors was developed by Valdés (2003). This model was obtained by means of homogeneous transformations, each component of the volumetric error can be described as the sum of different parts that are related to the geometric errors of the machine and to the corresponding Abbè offsets, Eq. (3-5). This model is based on the straightforwardness of application and adaptation of the homogeneous transformations to any kind of CMM and on the efficient diagnosis ability of the error synthesization method.

$$E_x = Pos(x) + Ry(x) + Rz(x) + [Ort(xy) + Yaw(x)] \cdot Y_{34} + [Ort(xz) + Pitch(x) + Yaw(z) + Roll(y)] \cdot (-Z - Z_{45}) + Roll(y) \cdot Z_{12} \quad (3)$$

$$E_y = Pos(y) + Ry(x) + Ry(z) + [Ort(xy) + Yaw(y)] \cdot (X_{23} + X) - Pitch(y) \cdot Z_{12} + -[Ort(yz) + Roll(x) + Pitch(y) + Pitch(z)] \cdot (-Z - Z_{45}) \quad (4)$$

$$E_z = Pos(z) + Rx(z) + Ry(z) - Roll(y) \cdot (X_{23} + X) - [Roll(x) + Pitch(y)] \cdot Y_{34} \quad (5)$$

where:

- $E_x$ ,  $E_y$  and  $E_z$  are the error components associated to each coordinate;
- $X$ ,  $Y$  and  $Z$  are the coordinates;
- $Pos(x)$ ,  $Pos(y)$  and  $Pos(z)$  are the positioning error at axis  $X$ ,  $Y$  and  $Z$ , respectively;
- $Rx(y)$  and  $Rx(z)$  are the straightness error of axis  $X$  direction  $Y$  and  $Z$ , respectively;
- $Ry(x)$  and  $Ry(z)$  are the straightness error of axis  $Y$  direction  $X$  and  $Z$ , respectively;
- $Rz(x)$  and  $Rz(y)$  are the straightness error of axis  $Z$  direction  $X$  and  $Y$ , respectively;
- $Pitch(x)$ ,  $Pitch(y)$  and  $Pitch(z)$  are the angular error Pitch at axis  $X$ ,  $Y$  and  $Z$ , respectively;
- $Yaw(x)$ ,  $Yaw(y)$  and  $Yaw(z)$  are the angular error Yaw to axis  $X$ ,  $Y$  and  $Z$ , respectively;
- $Roll(x)$  and  $Roll(y)$  are the angular error Roll at axis  $X$  and  $Y$ , respectively;
- $Y_{34}$ ,  $X_{23}$ ,  $Z_{12}$  and  $Z_{45}$  are the fixed offset;
- $Ort(xy)$ ,  $Ort(xz)$  and  $Ort(yz)$  are the orthogonality errors;

The input quantities, for once, may also be considered as measures that depend on other quantities. These values and their respective uncertainties may be obtained from a single observation or repeated observations, data supplied by the manufacturers of the instruments, observer's experience, literature, previous measurements, calibration standards, reference materials or calibration certificates, etc. According to the method used for evaluation of the numeric value of the uncertainties, these can be classified in: type A evaluation and type B evaluation.

The combined standard uncertainty can be calculated from the individual standard uncertainties of the variables that interfere on the measurement process, through a law known as "law of propagation of uncertainties".

In the equations (3 - 5) the law of propagation of uncertainty was applied, and equations (6 - 8) obtained.

$$\begin{aligned}
u_c^2 Ex = & \left( \frac{\partial Ex}{\partial Pos(x)} \right)^2 u_{Pos(x)}^2 + \left( \frac{\partial Ex}{\partial Ry(x)} \right)^2 u_{Ry(x)}^2 + \left( \frac{\partial Ex}{\partial Rz(x)} \right)^2 u_{Rz(x)}^2 + \left( \frac{\partial Ex}{\partial Ort(xy)} \right)^2 u_{Ort(xy)}^2 \cdot \left( \frac{\partial Ex}{\partial Y_{34}} \right)^2 u_{Y_{34}}^2 + \\
& + \left( \frac{\partial Ex}{\partial Yaw(y)} \right)^2 u_{Yaw(y)}^2 \cdot \left( \frac{\partial Ex}{\partial Y_{34}} \right)^2 u_{Y_{34}}^2 + \left( \frac{\partial Ex}{\partial Ort(xz)} \right)^2 u_{Ort(xz)}^2 \cdot \left( \frac{\partial Ex}{\partial (-Z-Z_{45})} \right)^2 u_{(-Z-Z_{45})}^2 + \left( \frac{\partial Ex}{\partial Pitch(x)} \right)^2 u_{Pitch(x)}^2 \cdot \\
& \cdot \left( \frac{\partial Ex}{\partial (-Z-Z_{45})} \right)^2 u_{(-Z-Z_{45})}^2 + \left( \frac{\partial Ex}{\partial Yaw(z)} \right)^2 u_{Yaw(z)}^2 \cdot \left( \frac{\partial Ex}{\partial (-Z-Z_{45})} \right)^2 u_{(-Z-Z_{45})}^2 + \left( \frac{\partial Ex}{\partial Ort(xz)} \right)^2 u_{Ort(xz)}^2 \cdot \\
& \cdot \left( \frac{\partial Ex}{\partial -Z-Z_{45}} \right)^2 u_{-Z-Z_{45}}^2 + \left( \frac{\partial Ex}{\partial Roll(y)} \right)^2 u_{Roll(y)}^2 \cdot \left( \frac{\partial Ex}{\partial (Z_{12}-Z-Z_{45})} \right)^2 u_{(Z_{12}-Z-Z_{45})}^2
\end{aligned} \tag{6}$$

$$\begin{aligned}
u_c^2 Ey = & \left( \frac{\partial Ey}{\partial Pos(y)} \right)^2 u_{Pos(y)}^2 + \left( \frac{\partial Ey}{\partial Rx(y)} \right)^2 u_{Rx(y)}^2 + \left( \frac{\partial Ey}{\partial Rz(y)} \right)^2 u_{Rz(y)}^2 + \left( \frac{\partial Ey}{\partial Ort(xy)} \right)^2 u_{Ort(xy)}^2 + \left( \frac{\partial Ey}{\partial X_{23}} \right)^2 u_{X_{23}}^2 + \left( \frac{\partial Ey}{\partial X} \right)^2 u_X^2 \\
& + \left( \frac{\partial Ey}{\partial Yaw(y)} \right)^2 u_{Yaw(y)}^2 \cdot \left( \frac{\partial Ey}{\partial (X_{23}+X)} \right)^2 u_{(X_{23}+X)}^2 - \left( \frac{\partial Ey}{\partial Pitch(y)} \right)^2 u_{Pitch(y)}^2 \cdot \left( \frac{\partial Ey}{\partial (Z_{12}-Z-Z_{45})} \right)^2 u_{(Z_{12}-Z-Z_{45})}^2 - \\
& - \left( \frac{\partial Ey}{\partial Ort(yz)} \right)^2 u_{Ort(yz)}^2 \cdot \left( \frac{\partial Ey}{\partial (-Z-Z_{45})} \right)^2 u_{(-Z-Z_{45})}^2 - \left( \frac{\partial Ey}{\partial Roll(x)} \right)^2 u_{Roll(x)}^2 \\
& \cdot \left( \frac{\partial Ey}{\partial (-Z-Z_{45})} \right)^2 u_{(-Z-Z_{45})}^2 - \left( \frac{\partial Ey}{\partial Pitch(z)} \right)^2 u_{Pitch(z)}^2 \cdot \left( \frac{\partial Ey}{\partial (-Z-Z_{45})} \right)^2 u_{(-Z-Z_{45})}^2
\end{aligned} \tag{7}$$

$$\begin{aligned}
u_c^2 Ez = & \left( \frac{\partial Ez}{\partial Pos(z)} \right)^2 u_{Pos(z)}^2 + \left( \frac{\partial Ez}{\partial Rx(z)} \right)^2 u_{Rx(z)}^2 + \left( \frac{\partial Ez}{\partial Ry(z)} \right)^2 u_{Ry(z)}^2 - \left( \frac{\partial Ez}{\partial Roll(y)} \right)^2 u_{Roll(y)}^2 \cdot \\
& \cdot \left( \frac{\partial Ez}{\partial (X_{23}+X)} \right)^2 u_{(X_{23}+X)}^2 - \left( \frac{\partial Ez}{\partial Roll(x)} \right)^2 u_{Roll(x)}^2 - \left( \frac{\partial Ez}{\partial Y_{34}} \right)^2 u_{Y_{34}}^2 - \left( \frac{\partial Ez}{\partial Pitch(x)} \right)^2 u_{Pitch(x)}^2 \cdot \left( \frac{\partial Ez}{\partial Y_{34}} \right)^2 u_{Y_{34}}^2
\end{aligned} \tag{8}$$

## 2.2. Determination of the uncertainty associated to the geometric errors

The aim of the present work is the calculation of the measurement uncertainty associated to the volumetric errors components in a CMM, at 20°C reference temperature. Each geometric error was measured individually and a mathematical model was developed for each one of them, in order to subsequently apply the law of propagation of uncertainties. The CMM, instrument and measuring device used remained in the room where the measurement was made during the necessary time to reach the thermal equilibrium. A detailed description of the model can be observed in Valdés (2005).

The results obtained during the estimate of the uncertainty associated to the geometric errors, in a measurement position, are summarized in the tables. The uncertainty values regarding the other errors are not presented because they are similar to the obtained values. For each evaluated error a Table is presented to show the expressions of the sensitivity coefficients and of the standard uncertainty of each influence variable, as well as, the distribution type, the degrees of freedom (D.F.) and the calculated value of standard uncertainty for the referred variable. These values, combined with standard uncertainty, effective degrees of freedom, coverage factor and expanded uncertainty were presented for evaluated geometric error.

### a) Measurement uncertainty of orthogonal errors

Equation (9) allows estimating the uncertainty associated to the measured orthogonal errors using the mechanical square standard and a LVDT type transducer.

$$Ort = L_{LVDT} + C_{Sq} + R_{LVDT} + L \cdot \alpha_{Sq} \cdot \Delta T_E \tag{9}$$

where:  $Ort$  is the orthogonal error;  $L_{LVDT}$  is the reading taken by LVDT;  $C_{Sq}$  is the correction due to error of the mechanical square;  $R_{LVDT}$  is the resolution of the LVDT;  $L$  is the conventional true value;  $\alpha_{Sq}$  is the coefficient of

thermal expansion of the mechanical square (granite) and  $\Delta T_{Sq}$  is the difference between the mechanical square temperature and the reference temperature.

Next, it has been applied a set of procedures for analysis of the standard uncertainties associated to the variables that influence the analyzed dimension. By applying the law of propagation of uncertainties in the Eq. (10), one can write:

$$u_c^2(Ort) = \left( \frac{\partial D}{\partial L_{LVDT}} \right)^2 (u_{L_{LVDT}})^2 + \left( \frac{\partial D}{\partial C_{Sq}} \right)^2 (u_{C_{Sq}})^2 + \left( \frac{\partial D}{\partial R_{LVDT}} \right)^2 (u_{R_{LVDT}})^2 + \left( \frac{\partial D}{\partial \alpha_{Sq}} \right)^2 (u_{\alpha_{Sq}})^2 + \left( \frac{\partial D}{\partial \Delta T_{Sq}} \right)^2 (u_{\Delta T_{Sq}})^2 \quad (10)$$

Similar results of the uncertainty associated to the square errors were obtained for all axes. The presence of small differences can be attributed to the operator that is in charge of the carriage movement, because the evaluated machine is manual. If the operator is not trained and extremely careful, he/she may produce strengths in the direction of the measured displacement, and this may consequently alter the measurement results. Table 1 presents the data regarding the calculation of the uncertainty of the orthogonal errors.

Table 1. Orthogonal error ( $Ort_{(XY)}$ ) measurement uncertainty analysis ( $Z=200$  mm).

Source of uncertainty	Uncertainty type	Probability distribution	Sensitivity coefficient	Degrees of freedom.	Standard uncertainty
$L_{LVDT}$	A	Normal	1	10	$5,0 \cdot E-4 \mu\text{m}$
$C_{Sq}$	B	Rectangular	1	$\infty$	$7,0 \cdot E-6 \mu\text{m}$
$R_{LVDT}$	B	Rectangular	1	$\infty$	$4,1 \cdot E-5 \mu\text{m}$
Combined standard uncertainty ( $u_c$ ) in $\mu\text{m}$					$5,0 \cdot E-4$
Effective degrees of freedom ( $v_{eff}$ )					193 (>100)
Coverage factor ( $v_{eff}$ , 95 %)					$k=2$
Expanded uncertainty ( $Up$ ) in $\mu\text{m}$					0,001

## b) Measurement uncertainty of positioning errors

Equation (11) allows determining the uncertainty associated to the measurement of positioning errors. This equation is based on the fact of that the positioning error is defined as being the difference between the reading value of the machine and the indicated value by the laser, which in this case is the standard. One can still incorporate to the model all the influence variables and the correction factors.

According to ISO/TR 16015 (2003), the uncertainty associated to the measurements of lengths due to thermal effects must consider the uncertainty associated to differential expansion between the measurand and the standard, the uncertainty associated to the measurement of temperature and the uncertainty associated to the variation of room temperature compared to the reference temperature Eq. (12).

$$E_{Pos} = M + R_{CMM} + R_L + Thermaleffect \quad (11)$$

$$E_{Pos} = M + R_{CMM} + R_L + \alpha_L L \Delta T_L + \alpha_E L \Delta T_E \quad (12)$$

where:  $E_{Pos}$  is the positioning error;  $M$  is the value indicated by machine;  $R_{CMM}$  is the resolution of the machine;  $R_L$  is the resolution of the laser;  $\Delta T_L$  is the difference between the room temperature and the reference temperature;  $\Delta T_E$  is the difference between the scale temperature and the reference temperature;  $\alpha_E$  and  $\alpha_L$  are the coefficients of thermal expansion of the scale (glass) and the laser beam, respectively.

Still, the laser interferometer system has the principle of measurement based on the wavelength of the light. So, room temperature variations cause changes in the wavelength of the light and thus, errors in the measurements are inserted. The calculation of the laser correction coefficient must be done for that the uncertainty can be estimated. Equation (13) sets a relation between wavelength, frequency and velocity of light, where:  $\lambda$  is the wavelength,  $v$  is the velocity of light and  $f$  is the frequency

$$\lambda = \frac{v}{f} \quad (13)$$

The velocity of light is constant in vacuum but, through the air, it varies as a function of air temperature, pressure and humidity. Since laser frequency is constant, the wavelength will change with the variation of the velocity of light. The distance  $D$  shown in the measurement display of the laser unity corresponds to the number of wavelengths,  $N$ , multiplied by a compensation factor,  $C$ , and the wavelength in the air,  $\lambda_A$ , as follows:

$$D = N \cdot C \cdot \lambda_A \quad (14)$$

The compensation factor  $C$  can be calculated by means of the equation below.  $N$  is the wavelength of movement and can be calculated using Eq. (15), where  $H$  is the humidity and  $P$  is the pressure.

$$C = \frac{10^{12}}{N + 10^{-6}} - 999000 \quad (15)$$

$$N = 0.3836391 \cdot P \cdot \left[ \frac{1 + 10^{-6} \cdot P(0.817 - 0.0133 \cdot T)}{1 + 0.003661 \cdot T} \right] - 3.033 \cdot 10^{-3} H(e^{0.057626T}) \quad (16)$$

Applying the law of propagation of uncertainties in Eq. (12), one can rewrite it as Eq. (17), which allows estimating the uncertainty associated to the positioning error.

$$u_c^2(E_{Pos}) = \left( \frac{\partial E_{Pos}}{\partial M} \right)^2 (u_c)^2 + \left( \frac{\partial E_{Pos}}{\partial R_{CMM}} \right)^2 (u_{R_{CMM}})^2 + \left( \frac{\partial E_{Pos}}{\partial R_L} \right)^2 (u_{R_L})^2 + \left( \frac{\partial E_{Pos}}{\partial \Delta T_L} \right)^2 (u_{\Delta T_L})^2 + \left( \frac{\partial E_{Pos}}{\partial \Delta T_E} \right)^2 (u_{\Delta T_E})^2 + \left( \frac{\partial E_{Pos}}{\partial \alpha_L} \right)^2 (u_{\alpha_L})^2 + \left( \frac{\partial E_{Pos}}{\partial \alpha_E} \right)^2 (u_{\alpha_E})^2 \quad (17)$$

Table 2 presents the data regarding the calculation of the uncertainty of the X-axis positioning errors.

### c) Measurement uncertainty of straightness errors and pitch and yaw angular errors

The mathematical model that represents the straightness errors, as well as, pitch and yaw angular errors, of all the axes, is given by Eq. (18).

$$R = e + R_L + C_L + Thermaleffect \quad (18)$$

Table 2. Positioning errors ( $Pos(x)$ ) measurement uncertainty analysis ( $X=100$  mm).

Source of uncertainty	Uncertainty type	Probability distribution	Sensitivity coefficient	Degrees of freedom	Standard uncertainty
$M$	A	Normal	1	4	8,1*E-2 $\mu\text{m}$
$R_{MM3c}$	B	Rectangular	1	$\infty$	1,2*E-6 $\mu\text{m}$
$R_L$	B	Rectangular	1	$\infty$	5,8 *E-3 $\mu\text{m}$
$\alpha_E$	B	Rectangular	6,4 *E-3 $\mu\text{m}^0\text{C}$	$\infty$	2,0*E-10 $^0\text{C}^{-1}$
$C_L$	B	Rectangular	6,4 *E-3 $\mu\text{m}^0\text{C}$	$\infty$	5,2*E-7 $^0\text{C}^{-1}$
$\Delta T$	B	Rectangular	1,4*E-16 $\mu\text{m}^0\text{C}$	$\infty$	0,4 $^0\text{C}$
Combined standard uncertainty ( $u_c$ ) in $\mu\text{m}$					8,1*E-2
Effective degrees of freedom ( $\nu_{eff}$ )					4,04
Coverage factor ( $\nu_{eff}$ , 95 %)					k=2,78
Expanded uncertainty ( $U_p$ ) in $\mu\text{m}$					0,2

Adding the terms related to the thermal effects and applying the law of propagation of uncertainties in Eq. (18), one can write Eq. (19).

$$u_c^2(R) = \left( \frac{\partial E}{\partial e} \right)^2 (u_c)^2 + \left( \frac{\partial E}{\partial R_L} \right)^2 (u_{R_L})^2 + \left( \frac{\partial E}{\partial C_L} \right)^2 (u_{C_L})^2 + \left( \frac{\partial E}{\partial \Delta T} \right)^2 (u_{\Delta T})^2 \quad (19)$$

where:  $R$  is the error;  $e$  is the indicated value by laser;  $R_L$  is the resolution of the laser;  $C_L$  is the coefficient of thermal expansion of the laser beam;  $\Delta T$  is the variation of the room temperature regarding the reference.

The data for calculation of the uncertainty associated to the  $X$ -axis straightness errors are presented in Tab. 3 and 4.

Table 3. Straightness error ( $Rx(y)$ ) measurement uncertainty analysis ( $X=275$  mm).

Source of uncertainty	Uncertainty type	Probability distribution	Sensitivity coefficient	Degrees of freedom	Standard uncertainty
$e$	A	Normal	1	4	0,2 $\mu\text{m}$
$R_L$	B	Rectangular	1	$\infty$	0,6*E-2 $\mu\text{m}$
$C_L$	B	Rectangular	1,8*E-6 $\mu\text{m}^0\text{C}$	$\infty$	4,6*E-5 $^0\text{C}^{-1}$
$\Delta T$	B	Rectangular	1,7*E-10 $\mu\text{m}^0\text{C}$	$\infty$	1,2 $^0\text{C}$
Combined standard uncertainty ( $u_c$ ) in $\mu\text{m}$					0,2
Effective degrees of freedom ( $v_{eff}$ )					4
Coverage factor ( $v_{eff}$ , 95 %)					k=2,78
Expanded uncertainty ( $Up$ ) in $\mu\text{m}$					0,6

Table 4. Straightness error ( $Rx(z)$ ) measurement uncertainty analysis ( $X=100$  mm).

Source of uncertainty	Uncertainty type	Probability distribution	Sensitivity coefficient	Degrees of freedom	Standard uncertainty
$e$	A	Normal	1	4	0,2 $\mu\text{m}$
$R_L$	B	Rectangular	1	$\infty$	0,6*E-3 $\mu\text{m}$
$C_L$	B	Rectangular	3,3*E-7 $\mu\text{m}^0\text{C}$	$\infty$	2,8*E-9 $^0\text{C}^{-1}$
$\Delta T$	B	Rectangular	1,1*E-19 $\mu\text{m}^0\text{C}$	$\infty$	0,3 $^0\text{C}$
Combined standard uncertainty ( $u_c$ ) in $\mu\text{m}$					0,2
Effective degrees of freedom ( $v_{eff}$ )					4
Coverage factor ( $v_{eff}$ , 95 %)					k=2,78
Expanded uncertainty ( $Up$ ) in $\mu\text{m}$					0,6

The found uncertainty values for the  $X$ -axis straightness errors have been similar in all the measurement positions and the Tab. 5 and 6 shows the data regarding the calculation of the uncertainty of the  $X$ -axis angular errors (pitch and yaw).

Table 5. Angular error ( $Pitch(x)$ ) measurement uncertainty analysis ( $X=200$  mm).

Source of uncertainty	Uncertainty type	Probability distribution	Sensitivity coefficient	Degrees of freedom	Standard uncertainty
$e$	A	Normal	1	4	1,6*E-7 $\mu\text{m}$
$R_L$	B	Rectangular	1	$\infty$	1,4*E-7 $\mu\text{m}$
$C_L$	B	Rectangular	7,8*E-6 $\mu\text{m}^0\text{C}$	$\infty$	2,2*E-9 $^0\text{C}^{-1}$
$\Delta T$	B	Rectangular	1,3*E-11 $\mu\text{m}^0\text{C}$	$\infty$	0,25 $^0\text{C}$
Combined standard uncertainty ( $u_c$ ) in $\mu\text{m}$					2,1*E-7
Effective degrees of freedom ( $v_{eff}$ )					12,4
Coverage factor ( $v_{eff}$ , 95 %)					k=2,17
Expanded uncertainty ( $Up$ ) in $\mu\text{m}$					4,6*E-7

Table 6. Angular error ( $Yaw(x)$ ) measurement uncertainty analysis ( $X=200$  mm).

Source of uncertainty	Uncertainty type	Probability distribution	Sensitivity coefficient	Degrees of freedom	Standard uncertainty
$e$	A	Normal	1	4	8,7*E-8 $\mu\text{m}$
$R_L$	B	Rectangular	1	$\infty$	1,4*E-7 $\mu\text{m}$
$C_L$	B	Rectangular	1,2*E-8 $\mu\text{m}^0\text{C}$	$\infty$	2,2*E-9
$\Delta T$	B	Rectangular	7,3*E-15 $\mu\text{m}^0\text{C}$	$\infty$	0,27
Combined standard uncertainty ( $u_c$ ) in $\mu\text{m}$					1,7*E-7
Effective degrees of freedom ( $v_{eff}$ )					51,5
Coverage factor ( $v_{eff}$ , 95 %)					k=2,01
Expanded uncertainty ( $Up$ ) in $\mu\text{m}$					3,4*E-7

#### d) Measurement uncertainty of roll angular error

The mathematical model of the roll angular error measurement is given by Eq. (20), where:  $Roll$  is the roll error;  $el$  is the indicated value by the electronic level;  $R_{Nb}$  is the resolution of the bubble level;  $R_{Ne}$  is the resolution of the electronic level and  $\Delta T$  is the variation of the room temperature regarding the reference.

$$Roll = el + R_{Nb} + R_{Ne} + Thermaleffect \quad (20)$$

By applying the law of propagation of uncertainties in Eq. (20), one can obtain the Eq. (21):

$$u_c^2(Roll) = \left(\frac{\partial E}{\partial el}\right)^2 (u_{el})^2 + \left(\frac{\partial E}{\partial R_{Nb}}\right)^2 (u_{R_{Nb}})^2 + \left(\frac{\partial E}{\partial R_{Ne}}\right)^2 (u_{R_{Ne}})^2 + \left(\frac{\partial E}{\partial \Delta T}\right)^2 (u_{\Delta T})^2 \quad (21)$$

The uncertainty values associated to the X-axis roll error measurement, Tab. 7, are very small, and thus, the contribution of this portion / part in the final uncertainty is practically insignificant.

Table 7. Angular error ( $Roll(x)$ ) measurement uncertainty analysis ( $X=200$  mm).

Source of uncertainty	Uncertainty type	Probability distribution	Sensitivity coefficient	Degrees of freedom	Standard uncertainty
$el$	A	Normal	1	4	$5,7 \cdot 10^{-7} \mu\text{m}$
$R_{Ne}$	B	Rectangular	1	$\infty$	$2,8 \cdot 10^{-7} \mu\text{m}$
$R_{Nb}$	B	Rectangular	1	$\infty$	$1,1 \cdot 10^{-5} \mu\text{m}$
$\Delta T$	B	Rectangular	$1,4 \cdot 10^{-5} \mu\text{m}/^\circ\text{C}$	$\infty$	$0,4 \cdot 10^{-1}$
Combined standard uncertainty ( $u_c$ ) in $\mu\text{m}$					$1,2 \cdot 10^{-5}$
Effective degrees of freedom ( $v_{eff}$ )					$\gg 100$
Coverage factor ( $v_{eff}$ , 95 %)					$k=2$
Expanded uncertainty ( $Up$ ) in $\mu\text{m}$					$2,4 \cdot 10^{-5}$

#### e) Measurement uncertainty of fixed offsets

The mathematical model of the fixed offsets measurement is:

$$FO = l + R_{RM} + l \cdot \alpha_{RM} \cdot \Delta T \quad (22)$$

where:  $FO$  is the fixed offset;  $l$  is the measured length;  $\alpha_{RM}$  is the coefficient of thermal expansion of mechanical rule;  $R_{RM}$  is the resolution mechanical rule and  $\Delta T$  is the room temperature variation. By applying the law propagation of uncertainty in the Eq. (23), one can write:

$$u_c^2(FO) = \left(\frac{\partial L}{\partial l}\right)^2 (u_l)^2 + \left(\frac{\partial L}{\partial R_{RM}}\right)^2 (u_{R_{RM}})^2 + \left(\frac{\partial L}{\partial \alpha_{RM}}\right)^2 (u_{\alpha_{RM}})^2 + \left(\frac{\partial L}{\partial \Delta T_{P/M}}\right)^2 (u_{\Delta T_{P/M}})^2 \quad (23)$$

The Table 8 shows the data regarding the calculation of the uncertainty of the offset  $Z_{12}$ .

Table 8. Fixed offset ( $Z_{12}$ ) measurement uncertainty analysis.

Source of uncertainty	Uncertainty type	Probability distribution	Sensitivity coefficient	Degrees of freedom	Standard uncertainty
$l$	A	Normal	1	4	0,2 mm
$R_m$	B	Rectangular	1	$\infty$	0,6 mm
$\alpha_{RM}$	B	Rectangular	$0,01 \text{ mm}/^\circ\text{C}$	$\infty$	$2,5 \cdot 10^{-8} \text{ }^\circ\text{C}$
$\Delta T_{p/m}$	B	Rectangular	$1 \text{ mm}/^\circ\text{C}$	$\infty$	$0,1 \text{ }^\circ\text{C}$
Combined standard uncertainty ( $u_c$ ) in mm					0,6
Effective degrees of freedom ( $v_{eff}$ )					420 ( $\gg 100$ )
Coverage factor ( $v_{eff}$ , 95 %)					$k=2$
Expanded uncertainty ( $Up$ ) in mm					1,2

### 2.3. Components of uncertainty of volumetric error

The value of the volumetric error components were estimated by means of the application of the developed synthesization equations. The volumetric error component in  $X$ -axis direction ( $E_x$ ) was calculated in various  $XY$  planes at fixed  $Z$  coordinate values. It was noticed that on the traced surfaces,  $E_x$  presented variation between 15 and 55  $\mu\text{m}$ . This component showed similar behavior at the evaluated planes, with a slight growing tendency along with the increasing of coordinate  $Y$ .

Next, uncertainties associated to the components of the volumetric error  $E_x$  were calculated (Fig. 3). It was observed that uncertainty values varied from 2,79 to 2,86  $\mu\text{m}$  and presented similar behavior at the different evaluated planes. The greatest influences upon the total uncertainty of the volumetric error  $E_x$  component were the orthogonality errors between axes  $X$ - $Y$  and  $X$ - $Z$  and  $Y$ -axis roll error. This fact is assured by the combination of error values and their uncertainties with values and uncertainties of fixed offsets, which are, in this case,  $Y_{3,4}$ ,  $Z_{4,5}$  and  $Y_{1,2}$ , respectively. The uncertainty values associated to the measurement of orthogonality errors and roll error were larger if compared to the other errors, which were measured with the laser interferometer.

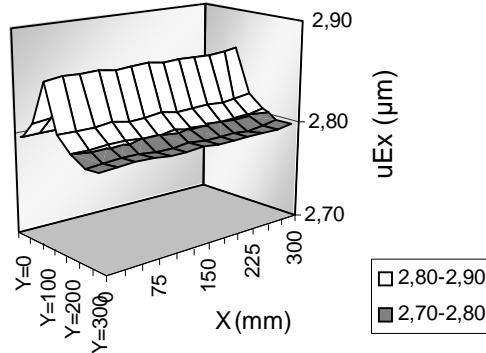


Figure 3. Uncertainty measurement of volumetric component  $E_x$ , to  $Y=150$  mm.

On the other hand, the values of the volumetric error components in  $Y$ -axis direction ( $E_y$ ) was estimated at various planes  $XY$ , for  $Z$  offsets of 125, 150, 175, 200, 225, 250 and 275 mm. The surfaces that describe the behavior of this component presented significant magnitude, taking values in the interval from  $-125$  to  $-300$   $\mu\text{m}$ . The increment of coordinate  $Z$  produced a considerable increase of component  $E_y$ , which is essentially due to the influence of orthogonality errors of axes  $Y$  and  $Z$ . Component  $E_y$  presents similar behavior over all evaluated plans. The uncertainty associated to the volumetric error component  $E_y$  presents nearly constant values, which vary between 4,00 and 4,03  $\mu\text{m}$  (Fig. 4). Component  $E_y$  presented the largest uncertainty values at reference temperature. This fact may be attributed to several factors: the synthesization equation of that component presenting a high number of influence variables; the orthogonality error magnitude between axes  $Y$  and  $Z$  and fixed offset  $Z_{1,2}$ , as well as the uncertainty associated to them.

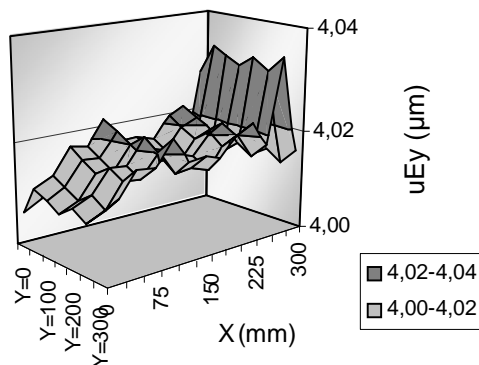


Figure 4. Uncertainty measurement of volumetric component  $E_y$ , to  $Z=150$  mm.

The volumetric error component in  $Z$ -axis direction was calculated for different  $ZX$  planes, as  $Y$  assumed values between 0 and 350 mm at 50 mm steps. The surfaces that describe the behavior of this component presented values in the interval from  $-7$  to 6  $\mu\text{m}$ . The uncertainty associated to the volumetric error component  $E_z$  presents small and nearly constant values, which vary between 1,98 and 2,00  $\mu\text{m}$  (Fig. 5).

Such values are smaller than the calculated uncertainty for  $E_x$  and  $E_y$  because of the reduced number of influence variables in the synthesization equation of  $E_z$ . Moreover, there are orthogonality errors in the referred equation. The fractions that presented the greatest influence over total uncertainty of component  $E_z$  were angular errors  $Roll(x)$  and  $Roll(y)$ . Mean and standard deviation values of  $E_z$  uncertainty are similar at different planes.

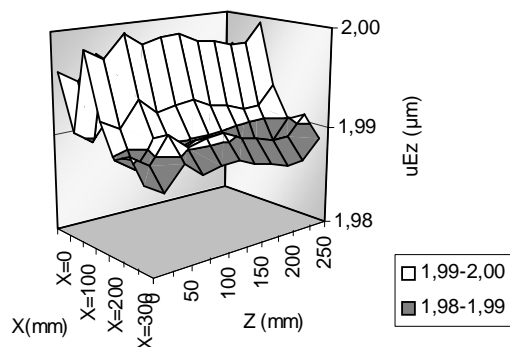


Figure 5. Uncertainty measurement of volumetric component  $E_z$ , to  $Y=150$  mm.

Mean and standard deviation of uncertainty values associated to components  $E_x$ ,  $E_y$  and  $E_z$  at the considered planes have shown that uncertainty has homogeneous behavior. Therefore, it can be said that at any point in the work volume of the CMM, the components of volumetric error present uncertainty values close to 2,8, 4,0 and 2,0  $\mu\text{m}$ , respectively.

### 3. CONCLUSIONS

In the end of this work, the following conclusions may be presented.

The procedures described in ISO GUM have been efficient to determine the uncertainty associated the components of the volumetric error at any point of the work volume of the evaluated machine at given conditions. By determining the effects of variables in three-dimensional uncertainty information was obtained.

The uncertainties associated to the components of the volumetric error ( $E_x$ ,  $E_y$  and  $E_z$ ) at 20°C were homogeneously perceived at several planes. It values close to 2,8, 4,0 and 2,0  $\mu\text{m}$ , respectively.

The Measuring Machines performance is affected by several factors due to its structural complexity, so much that the calculation of the uncertainty becomes a very tiring task.

The positioning errors are affected by a larger number of uncertainty sources when compared to the other geometric errors.

The uncertainty associated to the temperature variation has been a factor that contributed significantly for the uncertainties associated to the angular error measurement of CMM. For positioning, straightness and orthogonal errors the uncertainty associated to the variability of measurement was more significant.

The values of uncertainties associated to the thermal effects are higher than those calculated for other influence variables, however pondered by very small coefficients, are little significant for the total uncertainty of the evaluated geometrical error.

Although the uncertainties associated to the coefficients of thermal expansion have also been pondered by the coefficients that vary with the used value as standard, they have not been relevant because were much lower than other considered uncertainties.

The influence variables which contributed more significantly in the uncertainty of the components of the volumetric error were: magnitude of the fixed offsets and the orthogonality errors, as well as the uncertainty associated to them.

### 4. ACKNOWLEDGEMENT

The authors are grateful to FAPESP - Fundação de Amparo à Pesquisa do Estado de São Paulo, by the financial support in this work, Process number 98/15436-7 and 03/11453-4.

### 5. REFERENCES

- Balsamo, A.M., Di Ciommo, R., Mugno, B.I., Rebaglia, E. Ricci, and Grella, R., 1999, "Evaluation of CMM uncertainty through Monte Carlo simulations", Annals of the CIPR 48(1), pp 425-428.
- Bosch, J.A., 1995, "Coordinate measuring machines and system". New York: Marcel Dekker, 444 p.
- ISO TAG 4/WG 3, 1993, "Guide to the Expression of Uncertainty in measurement" (GUM), Geneva: International Organization for Standardization (ISO), 134 p.
- ISO/TR 16015, 2003, "Geometrical product specifications (GPS) – Systematic errors and contributions to measurement uncertainty of length measurement due to thermal influences", Technical report.
- Valdés, R.A., 2003, "Modelo de Sintetização de Erros Termicamente Induzidos em MM3Cs", Tese (Doutorado) - Escola de Engenharia de São Carlos, Universidade de São Paulo, São Carlos, Brazil, 190 p.
- Valdés, R.A., 2005, "Cálculo da incerteza em MM3C considerando às influências térmicas", Relatório FAPESP. Processo N. 03/11453-4 - Escola de Engenharia de São Carlos, Universidade de São Paulo, São Carlos, S.Paulo, Brazil, 117 p.